Title
Unit firing and oscillations at seizure onset in epileptic rodents.

Authors
Li, Lin
Bragin, Anatol
Staba, Richard
et al.

Publication Date
2019-07-01

DOI
10.1016/j.nbd.2019.03.027

Peer reviewed

HHS Public Access

Author manuscript

Neurobiol Dis. Author manuscript; available in PMC 2020 July 01.

Published in final edited form as:

Neurobiol Dis. 2019 July ; 127: 382–389. doi:10.1016/j.nbd.2019.03.027.

Unit firing and oscillations at seizure onset in epileptic rodents

Lin Li[a], **Anatol Bragin**[a,b], **Richard Staba**[a], **Jerome Engel jr**[a,b,c,d,*]

[a]Department of Neurology, University of California, Los Angeles, CA, USA

[b]Brain Research Institute, University of California, Los Angeles, CA, USA

[c]Department of Neurobiology, David Geffen School of Medicine at UCLA, Los Angeles, CA, USA

[d]Department of Psychiatry and Biobehavioral Sciences, David Geffen School of Medicine at UCLA, Los Angeles, CA, USA

Abstract

Epileptic seizures result from a variety of pathophysiological processes, evidenced by different electrographic ictal onset patterns, as seen on direct brain recordings. The two most common electrographic patterns of focal ictal onset in patients are hypersynchronous (HYP) and low-voltage fast (LVF). Whereas LVF ictal onsets were believed to result from disinhibition; based on similarities with absence seizures, focal HYP ictal onsets were believed to result from increased synchronizing inhibition. Recent findings, however, suggest the differences between these seizure onset types are more complicated and, in some cases, the opposite of these concepts are true. The following review presents evidence that a reduction of tonic inhibition on small pathologically interconnected neuron (PIN) clusters generating pathological high-frequency oscillations (pHFOs), which reflect abnormal synchronously bursting neurons may be the cause of HYP ictal onsets. Increased inhibition preceding LVF ictal onsets are discussed in other reviews in this issue. We postulate that neuronal cell loss following epileptogenic insults can result in structural reorganization, giving rise to small PIN clusters, which generate pHFOs. These clusters have a heterogeneous distribution and are spatially stable over time. Studies have demonstrated that a transient reduction in tonic inhibition causes these clusters to increase in size. This could result in consolidation and synchronization of pHFOs until a critical mass leads to propagation of HYP ictal discharges. Viewed within a network neuroscience framework, local disturbances such as PIN clusters are likely to contribute to large-scale brain network alterations: a better understanding of these epileptogenic networks promises to elucidate mechanisms of ictogenesis, epileptogenesis, and certain comorbidities of epilepsy.

1. Introduction

The two most common electrographic patterns of ictal onset in patients, as recorded with intracranial electrodes, are hypersynchronous (HYP) and low-voltage fast (LVF), characterized respectively by repetitive high amplitude isolated discharges, and a buildup of gamma activity, referred to as a recruiting rhythm (Engel, 2013; Ogren et al., 2009a; Perucca

*Corresponding author at: Department of Neurology, David Geffen School of Medicine at UCLA, 710 Westwood Plaza, Los Angeles, CA 90095-1769, USA. engel@ucla.edu (J. Engel).

et al., 2014; Velasco et al., 2000) (Fig. 1). In patients, HYP ictal onsets are most commonly seen with limbic seizures, particularly originating in hippocampus, while LVF ictal onsets are more often seen in seizures originating in neocortex (Memarian et al., 2015; Velasco et al., 2000). Both types of ictal onsets are encountered in common rodent models of mesial temporal lobe epilepsy (MTLE), such as those following status epilepticus induced by pilocarpine and kainic acid (Bragin et al., 2005; Bragin et al., 1999c; Huberfeld et al., 2011; Lévesque et al., 2012; Merricks et al., 2015; Truccolo et al., 2011; Weiss et al., 2016b). Earlier studies of acute epileptic seizures induced in feline neocortex by local application of penicillin suggested that LVF ictal onsets resulted from the gradual disappearance of a protective after-hyperpolarization, reflected as the slow wave of interictal spike-and wave complexes, and its replacement by a prolonged after-depolarization (Matsumoto and Ajmone Marsan, 1964b). Conversely, because of the electrographic resemblance of HYP ictal onsets to the generalized spike-and-wave of absence seizures, which depend on increased inhibitory input to produce the hypersynchronization (de Curtis and Avoli, 2016; Lévesque et al., 2012), it was suggested that HYP seizures reflect enhanced inhibitory mechanisms (Engel et al., 2007). Recent studies indicate that the differences between the two ictal onset types may not be so straightforward, and the opposite in some cases may be true for both seizure onset patterns. Several studies, reviewed in other chapters in this issue, provide evidence that LVF ictal onsets in neocortex originate with enhanced inhibition (De Curtis et al., this issue, Weiss et al., this issue), while this review will focus on evidence that HYP ictal onsets in rats, induced by intrahippocampal kainic acid, may be the result of decreased tonic inhibition in neuronal clusters that generate pathological high-frequency oscillations (pHFOs).

2. Pathological high-frequency oscillations

High-frequency oscillations (HFOs) are brief bursts of EEG activity in the range of 80 to 600 Hz (Buzsaki et al., 1992; Buzsáki and Silva, 2012; Jefferys et al., 2012; Menendez de la Prida and Trevelyan, 2011). Physiological HFOs in the range of 80 to 200 Hz, termed ripples, have been well described in normal hippocampus (Buzsaki, 2015; Buzsaki et al., 1992; Ylinen et al., 1995). Studies suggest ripples predominantly reflect summated inhibitory postsynaptic potentials (IPSPs), which serve to synchronize neuronal activity over wide areas and are important for information transfer and memory consolidation (Buzsaki, 2015; Buzsáki and Silva, 2012). Physiological ripples also involve coherent action potential firing in a subset of cells, which can lend a spikey appearance to the local field potential (LFP) (Csicsvari et al., 2000; Valero et al., 2017).

Given the view that HYP seizures could arise from enhanced synchronizing inhibition (Engel et al., 2007) once ripples were identified as reflecting summated IPSPs, it was of great interest to determine the characteristics of these HFOs in epileptic hippocampus, compared to the contralateral hippocampus. Studies were first carried out in the intrahippocampal kainate rat model of mesial temporal lobe epilepsy. They revealed no appreciable change in HFOs in the contralateral hippocampus, but the appearance of even faster HFOs in the lesioned hippocampus, which were then referred to as fast ripples (FRs) (Bragin et al., 1999b; Bragin et al., 2002; Bragin et al., 2007). In other studies, it was shown that in the epileptic hippocampus normal HFOs coexist with pathological (Alvarado-Rojas et

al., 2014; Valero et al., 2017). Subsequently, it became clear that these oscillations, with a frequency range as high as 600 Hz, were identified only in regions capable of generating spontaneous seizures, and were, therefore, considered to be indicators of the pathological substrate of ictogenesis in mesial temporal structures (Bragin et al., 1999a; Engel Jr et al., 2009; Staba et al., 2002).

Subsequent studies demonstrated that fast ripples did not reflect summated IPSPs, but rather summated action potentials of abnormal synchronously bursting neurons (Bragin et al., 2007; Engel Jr et al., 2009) (Fig. 2), which represent the fundamental neuronal mechanism underlying epileptiform interictal EEG spikes (Matsumoto and Ajmone Marsan, 1964a), as well as hypersynchronous ictal onsets (Bragin et al., 2009; Bragin et al., 2005). Whereas this synchronous bursting activity was reported to characterize up to 90% of neurons within the feline neocortical acute penicillin focus (Matsumoto and Ajmone Marsan, 1964a), it has been difficult to demonstrate such synchronously bursting units in patients with mesial temporal lobe epilepsy, or in chronic rodent models, where only approximately 5% of neurons exhibit this synchronously bursting activity (Babb et al., 1981; Bragin et al., 2011; Valero et al., 2017). Fortunately, however, the LFPs generated by this synchronous activity is easily recorded with microelectrodes, and also clinical electrodes (Jacobs et al., 2008; Jirsch et al., 2005; Worrell et al., 2008; Worrell et al., 2004), in patients, as well as rodents, making it a useful biomarker of the epileptogenic region in patients who are candidates for surgical resection (Engel Jr and da Silva, 2012; Jacobs et al., 2012; Jacobs et al., 2010; van't Klooster et al., 2011).

Initial studies suggested that pHFOs could be distinguished from normal high-frequency oscillations on the basis of frequency; ripples being normal and fast ripples being abnormal. However, further studies of microelectrode recordings in dentate gyrus of epileptic hippocampus in rats, following intrahippocampal kainate, revealed ripple frequency HFOs, which are not generated by normal dentate gyrus (Bragin et al., 2002; Engel Jr et al., 2009). This clearly indicated that ripple frequency HFOs are not always normal, but that some also reflect pathological bursting neurons.

Fast ripple oscillations in hippocampus appear to always be pHFOs, while ripple frequency oscillations maybe pHFOs, or normal HFOs. In contrast, normal HFOs in the fast ripple frequency range do occur in eloquent neocortical regions such as motor cortex, sensory cortex, language cortex, and visual cortex. Frequency, therefore, does not determine pathogenicity (Engel Jr et al., 2009). Consequently, frequency does not distinguish normal from pathological high frequency oscillations, and the term *pathological high frequency oscillations* was introduced as a better description of the epileptogenic abnormality (Aivar et al., 2014; Engel Jr et al., 2009; Ibarz et al., 2010).

In rat experiments, pHFOs can be recorded following epileptogenic insults weeks before spontaneous seizures appear, and only in animals that later develop epilepsy (Bragin et al., 2004). This strongly suggests they reflect epileptogenic, as well as ictogenic mechanisms and are not the result of seizures.

3. Structural correlations

Correlation of microelectrode recordings with hippocampal pathology from epileptic rats shows pHFOs occur in perilesional areas and correlate with cell loss in some, but not all, models of epilepsy (Bragin et al., 1999b; Bragin et al., 2000b; Foffani et al., 2007; Jiruska et al., 2010). In patients with MTLE, registration of microelectrode recordings with MRI indicate that pHFOs preferentially occur in areas with atrophy (Ogren et al., 2009b; Staba et al., 2007; Staba et al., 2004) (Fig. 3), suggesting that they are the result of an initial precipitating insult which causes cell loss, followed by the neuronal reorganization responsible for epileptogenesis. This would include sprouting of excitatory and inhibitory neurons, loss of dendritic domain such that axonal input is closer to the axon hillock, and aberrant reconnections that all predisposed to hypersynchronization (Engel et al., 2007). Roles for antidromic firing (Bahner et al., 2011; Gutnick and Prince, 1972) as well as gap junctions (Draguhn et al., 1998; Schmitz et al., 2001; Simon et al., 2013) have been suggested for both normal and pHFOs.

An important part of this structural reorganization presumably underlying the generation of pHFOs is that these-generating neuron clusters are not homogeneously distributed throughout structures, such as the hippocampus, but, rather, localized to small clusters of neurons, referred to as pathologically interconnected neuron clusters (PIN clusters). PIN clusters are imbedded within more normally functioning brain structure. This has been demonstrated by microelectrode recordings in hippocampus of the intrahippocampal kainate rat (Bragin et al., 2002) and in patients with mesial temporal lobe epilepsy. In the latter, the pin clusters are associated with localized patches of atrophy identified by voxel-based morphometry (Staba et al., 2012). Furthermore, in rats, these PIN clusters have been shown to be spatially stable over time (Bragin et al., 2003). The existence of this organization suggests a novel mechanism for ictogenesis in MTLE.

4. The PIN Cluster hypothesis

Previous work in our laboratory, and others, had suggested that inhibition is increased in the epileptic hippocampus in patients and rats, consistent with the former view that enhanced inhibition is necessary for the generation of HYP ictal onsets (Engel Jr., 1995; Wilson et al., 1998). One particular series of studies demonstrating enhanced inhibition in the epileptic hippocampus is the observation that paired pulse stimulation of perforant path, the primary input from entorhinal cortex to hippocampus, which normally results in enhancement of the response to the second stimulation, causes prolonged suppression of the second response in patients with MTLE (Wilson et al., 1998), as well as rodents with experimental mesial temporal epilepsy (Bragin et al., 2002). This was taken to reflect an enhanced inhibitory response to the first stimulation, which could be a protective mechanism, or could contribute to the hypersynchrony responsible for ictogenesis.

Although paired-pulse suppression is characteristic of the epileptic hippocampus in patients and rats, when the recording electrodes are in a PIN cluster in rats, the second pulse produces an enhanced response, and often pHFOs (Bragin et al., 2002) (Fig. 4), suggesting that, whereas there is increased inhibition in the epileptic hippocampus in general, within

PIN clusters, inhibition is actually decreased. Although PIN clusters are generally spatially stable over time (Bragin et al., 2003), introduction of bicuculline causes them to increase in size (Bragin et al., 2002) (Fig. 5), indicating that loss of tonic inhibition, for a variety of reasons, might cause PIN clusters to increase in size, consolidate, and synchronize until a critical mass effect causes the hypersynchronous discharge to propagate, resulting in a seizure (Bragin et al., 2009; Bragin et al., 2005). This hypothesized mechanism of ictogenesis is supported by the fact that there is a positive correlation between seizure frequency and PIN cluster density in the hippocampus of intrahippocampal kainate rats (Bragin et al., 2004), and in these animals (Bragin et al., 2005), as well as in patients with mesial temporal lobe epilepsy (Weiss et al., 2016a; Weiss et al., 2016b), there is an increase in amplitude and duration of pHFOs leading up to a seizure. This suggests that while the hypersynchrony of HYP ictal onsets may require phasic inhibition, the generation of these seizures are brought about by decreased tonic inhibition on pHFOs within PIN clusters; at some point, this process evolves into HYP ictal discharges that can propagate. Indeed, each hypersynchronous discharge of a HYP ictal onset in kainate rats consists of a pHFO followed by a tail gamma wave, referred to as a pHFO-tail gamma complex (Bragin et al., 1999c). These events are stereotyped during the hypersynchronous seizure, which, in patients with mesial temporal lobe epilepsy, may or may not be associated with an aura. Often, in patients, the depth electrode-recorded HYP seizure terminates spontaneously, causing an aura in isolation, or perhaps no symptoms, in which case it would be an electrographic seizure (Engel et al., 2007). The HYP ictal discharge, however, can transform into an LVF pattern, during which contralateral propagation occurs, associated with a typical limbic seizure with impaired awareness (Engel et al., 2007). The mechanism by which this transition occurs is not known – it could reflect involvement of adjacent cortex, in which case the LVF ictal onset would be generated in a separate structure; however, in the intrahippocampal kainate rat, both HYP and LVF ictal onsets can be recorded from the same hippocampal electrodes.

A role for PIN clusters and pHFOs in the generation of LVF seizures in neocortex has not been demonstrated and, as mentioned earlier, there is increasing evidence that LVF seizures are initiated by increased activity in inhibitory interneurons (De Curtis et al., this issue, Weiss et al., this issue). Occasionally, however, there is a single herald spike preceding the LVF onset, and this spike is associated with pHFOs (de Curtis and Avoli, 2016; Levésque et al., 2011). It is possible, therefore, that LVF seizures are initially precipitated by mechanisms involving expansion of PIN clusters, as with HYP ictal onsets, and that the subsequent increase in inhibitory activity is an initial protective reaction in adjacent tissue, which then results in rebound excitation and an LVF seizure. Indeed, at least one LVF seizure recorded with clinical electrodes in a patient was preceded by a microelectrode-recorded HYP seizure which was not visible to the clinical electrodes (Weiss et al., 2016a) (Fig. 6). It is possible, therefore, that at least some apparent LVF ictal onsets are actually HYP onsets occurring at a distance from the recording contacts.

5. The epileptogenic network

There is increasing interest in mechanisms of epileptogenesis, as opposed to ictogenesis, and the potential importance of an epileptogenic network. Recent work has emphasized the

concept of modeling the brain as a complex system in order to understand the epileptogenic network (Scott et al., 2018). As part of this concept, disturbed signaling pathways and local circuit activity can be associated with an alteration in large-scale brain activity and changes in the behavioral phenotype. In practice, even the local disturbances in excitatory or inhibitory mechanisms, or both, could cause network changes that contribute to epileptogenesis. For example, pHFOs occur early following intrahippocampal kainate in rats, but only in those animals that subsequently develop spontaneous seizures (Bragin et al., 2004). Another study showed pHFOs can be recorded early in rats that subsequently develop epilepsy after fluid percussion injury (FPI) (Bragin et al., 2016). They are, therefore, a likely biomarker of epileptogenesis and reflect the epileptogenic mechanism. Furthermore, the timing of the appearance of pHFOs correlates with the timing of spontaneous seizures – that is, the earlier that pHFOs occur, the earlier that subsequent spontaneous seizures occur (Bragin et al., 2004).

More recently, studies have revealed that pHFOs occur widely throughout the brain during the course of epileptogenesis caused by FPI (Li et al., 2018; Sheybani et al., 2018). pHFOs occurring at the lesion site do not necessarily predict which animals will develop epilepsy, but those that subsequently occur in multiple other areas do predict which animals will eventually develop spontaneous seizures (Li et al., 2018; Sheybani et al., 2018) (Fig. 7). This strongly suggests the development of a PIN cluster network during epileptogenesis that is necessary to support the initiation of spontaneous ictogenesis. Hippocampal pHFOs can also trigger spindles in remote limbic areas that might not only contribute to epileptogenesis, but also interfere with processes involved with memory consolidation (Gelinas et al., 2016). This deleterious effect is similar to the distortion of physiological ripples for memory consolidation (Valero et al., 2017). A similar network-level effect can also be found in the thalamo-cortical circuit (Ding et al., 2011). In addition to traditional approaches that focus on genes or synapses, understanding of epileptogenic networks may lead to the development of novel diagnostic and therapeutic strategies. An identified epileptogenic network at the macro- and micro levels, for example, could then be targeted with an intervention that manipulates neural networks in such a way that either prevents seizures or pushes the network into a different dynamic pattern that is less likely to generate seizures.

6. Posttraumatic epilepsy after traumatic brain injury

Similar to the intrahippocampal kainate rat model, recent studies found evidence of neuronal hyperexcitability in the FPI model of human closed-head injury, including evidence for pHFOs as an electrophysiological biomarker of post-traumatic epilepsy (PTE) (Bragin et al., 2016; Engel Jr., 2019; Pitkanen and Engel Jr., 2014; Pitkanen and Immonen, 2014; Reid et al., 2016). In FPI rats that develop PTE, pHFOs with frequencies between 80 and 600 Hz, and duration from 10 to 40, milliseconds, can be recorded in perilesional neocortex, which are the same areas where seizures begin (Bragin et al., 2016; Reid et al., 2016). In these PTE studies, a new electrophysiological pattern, termed repetitive pHFOs and EEG spikes (rHFOSs), was identified; it consists of a 10 to 16 Hz arcuate-shaped rhythm of EEG spikes with superimposed pHFOs (Fig. 8). rHFOSs occurred within the first 2 weeks after FPI, were found in a greater number of rats with severe than mild FPI, their rate of occurrence decreased from earlier to later recordings after FPI, and they were only found in rats that

later developed spontaneous focal seizures (Bragin et al., 2016; Reid et al., 2016). The arcuate pattern of rHFOSs distinguishes it from other common EEG patterns, such as spike-wave discharges (SWDs) and sleep spindles. The frequency of SWDs are lower (6–9 Hz) than rHFOSs and do not contain pHFOs. The rHFOSs can be recorded by screw electrodes in skull during sleep and wakefulness, while the SWDs and sleep spindles can only be measured during sleep (Bragin et al., 2016). The low frequency oscillations of rHFOSs can be recorded with conventional EEGs (i.e. sampling rate 200 Hz), while pHFOs require higher sampling rates. These results and the features of rHFOSs make these EEG events a potential non-invasive biomarker of epileptogenesis.

The temporal and spatial patterns of pHFOs after FPI are similar to those in the status epilepticus model (Bragin et al., 1999b; Bragin et al., 2016; Bragin et al., 2000a; Bragin et al., 2002; Bragin et al., 2004; Reid et al., 2016). One difference, however, is that in the FPI model pHFOs are not only associated with hippocampal sharp-waves, but also generated within rHFOSs. The mechanism of rHFOSs is unknown, but recordings show the largest spikes of the rHFOSs are triggered by an increase in multiunit activity (Bragin et al., 2016). This finding suggests rHFOSs are generated from hypersynchronous neuronal discharges, which are similar to the local synchronous bursting associated with pHFOs in the kainate lesioned hippocampus. In both models, the neuronal substrates of epileptogenesis could be caused by the formation of widespread PIN clusters.

7. Summary

Previously held beliefs regarding the underlying mechanisms of two of the most common patterns of ictal onset, LVF and HYP, have been challenged by recent work using sophisticated single neuron stimulation and recording techniques. The prevailing consensus was that LVF ictal onset was mediated by a gradual disappearance of protective inhibition, and HYP ictal onset was mediated by increased synchronizing inhibitory mechanisms. The recently emerging series of findings shows that LVF onsets can be preceded by increased inhibitory activity, whereas HYP ictal onsets could arise from decreased tonic inhibition. There is compelling evidence that pHFOs reflect summated action potentials of abnormal synchronously bursting neurons arranged in small, spatially stable, PIN clusters, imbedded within more normal tissue.. Reduction of tonic inhibition within PIN clusters results in an increase in their size, consolidation and synchronization of the pHFOs, suggesting a mechanism for ictogenesis (Fig. 9). New studies have also recorded neocortical pHFOs in rats that develop PTE, suggesting the mechanisms generating seizures, are similar following status epilepticus and TBI. Additional evidence implicates pHFOs and PIN cluster networks in the mechanisms of epileptogenesis and some comorbidities of epilepsy, making this a fruitful direction for future research.

Acknowledgments

This study was supported by National Institutes of Health, USA (R01-NS065877, R01-NS033310, R01-NS106957, and U54-NS100064).

References

Aivar P, et al., 2014 Extracellular calcium controls the expression of two different forms of ripple-like hippocampal oscillations. J. Neurosci 34, 2989–3004. [PubMed: 24553939]

Alvarado-Rojas C, et al., 2014 Slow modulations of high-frequency activity (40–140-Hz) discriminate preictal changes in human focal epilepsy. Sci. Rep 4, 4545. [PubMed: 24686330]

Babb TL, et al., 1981 Neuronal firing patterns during the spread of an occipital lobe seizure to the temporal lobes in man. Electroencephalogr. Clin. Neurophysiol 51, 104–107. [PubMed: 6161774]

Bahner F, et al., 2011 Cellular correlate of assembly formation in oscillating hippocampal networks in vitro. Proc. Natl. Acad. Sci. U. S. A 108, E607–E616. [PubMed: 21768381]

Bragin A, et al., 1999a High-frequency oscillations in human brain. Hippocampus. 9, 137–142. [PubMed: 10226774]

Bragin A, et al., 1999b Hippocampal and entorhinal cortex high-frequency oscillations (100–500 Hz) in human epileptic brain and in kainic acid-treated rats with chronic seizures. Epilepsia. 40, 127–137. [PubMed: 9952257]

Bragin A, et al., 1999c Electrophysiologic analysis of a chronic seizure model after unilateral hippocampal KA injection. Epilepsia. 40, 1210–1221. [PubMed: 10487183]

Bragin A, et al., 2000a Local generation of fast ripples in epileptic brain. Parallel in vivo and in vitro studies. Soc. Neurosci. Abstr 26 (part 1), 227 New Orleans.

Bragin A, et al., 2000b Chronic epileptogenesis requires development of a network of pathologically interconnected neuron clusters: a hypothesis. Epilepsia. 41, S144–S152. [PubMed: 10999536]

Bragin A, et al., 2002 Local generation of fast ripples in epileptic brain. J. Neurosci 22, 2012–2021. [PubMed: 11880532]

Bragin A, et al., 2003 Spatial stability over time of brain areas generating fast ripples in the epileptic rat. Epilepsia. 44, 1233–1237. [PubMed: 12919396]

Bragin A, et al., 2004 High-frequency oscillations after status epilepticus: epileptogenesis and seizure genesis. Epilepsia. 45, 1017–1023. [PubMed: 15329064]

Bragin A, et al., 2005 Analysis of chronic seizure onsets after intrahippocampal kainic acid injection in freely moving rats. Epilepsia. 46, 1592–1598. [PubMed: 16190929]

Bragin A, et al., 2007 Voltage depth profiles of high-frequency oscillations after kainic acid-induced status epilepticus. Epilepsia. 48, 35–40.

Bragin A, et al., 2009 The cause of the imbalance in the neuronal network leading to seizure activity can be predicted by the electrographic pattern of the seizure onset. J. Neurosci 29, 3660–3671. [PubMed: 19295168]

Bragin A, et al., 2011 Further evidence that pathologic high-frequency oscillations are bursts of population spikes derived from recordings of identified cells in dentate gyrus. Epilepsia. 52, 45–52.

Bragin A, et al., 2016 Pathologic electrographic changes after experimental traumatic brain injury. Epilepsia. 57, 735–745. [PubMed: 27012461]

Buzsaki G, 2015 Hippocampal sharp wave-ripple: a cognitive biomarker for episodic memory and planning. Hippocampus. 25, 1073–1188. [PubMed: 26135716]

Buzsáki G, Silva F.L.d., 2012 High frequency oscillations in the intact brain. Prog. Neurobiol 98, 241–249. [PubMed: 22449727]

Buzsaki G, et al., 1992 High frequency network oscillation in the hippocampus. Science. 256, 1025–1027. [PubMed: 1589772]

Csicsvari J, et al., 2000 Ensemble patterns of hippocampal CA3-CA1 neurons during sharp wave-associated population events. Neuron. 28, 585–594. [PubMed: 11144366]

de Curtis M, Avoli M, 2016 GABAergic networks jump-start focal seizures. Epilepsia. 57, 679–687. [PubMed: 27061793]

Ding M-C, et al., 2011 Cortical excitation and inhibition following focal traumatic brain injury. J. Neurosci 31, 14085–14094. [PubMed: 21976493]

Draguhn A, et al., 1998 Electrical coupling underlies high-frequency oscillations in the hippocampus in vitro. Nature. 394, 189–192. [PubMed: 9671303]

Engel JJ, 2013 Seizures and Epilepsy, second edition Oxford University Press, New York.

Engel J Jr., da Silva FL, 2012 High-frequency oscillations – where we are and where we need to go. Prog. Neurobiol 98, 316–318. [PubMed: 22342736]

Engel J Jr., et al., 2009 High-frequency oscillations: what is normal and what is not? Epilepsia. 50, 598–604. [PubMed: 19055491]

Engel J Jr., 1995 Inhibitory mechanisms of epileptic seizure generation. Adv. Neurol 67, 157–171. [PubMed: 8848967]

Engel J Jr., 2019 Epileptogenesis, traumatic brain injury, and biomarkers. Neurobiol. Dis 123, 3–7. [PubMed: 29625256]

Engel JJ, Dichter MA, Schwartzkroin PA, 2007 Basic mechanisms of human epilepsy In: Engel J Jerome, Pedley, Timothy A (Eds.), Epilepsy: A Comprehensive Textbook. Wolters Kluwer/ Lippincott Williams & Wilkins, pp. 495–508.

Foffani G, et al., 2007 Reduced spike-timing reliability correlates with the emergence of fast ripples in the rat epileptic hippocampus. Neuron. 55, 930–941. [PubMed: 17880896]

Gelinas JN, et al., 2016 Interictal epileptiform discharges induce hippocampal-cortical coupling in temporal lobe epilepsy. Nat. Med 22, 641–648. [PubMed: 27111281]

Gutnick MJ, Prince DA, 1972 Thalamocortical relay neurons: antidromic invasion of spikes from a cortical epileptogenic focus. Science. 176, 424–426. [PubMed: 4337289]

Huberfeld G, et al., 2011 Glutamatergic pre-ictal discharges emerge at the transition to seizure in human epilepsy. Nat. Neurosci 14, 627–634. [PubMed: 21460834]

Ibarz JM, et al., 2010 Emergent dynamics of fast ripples in the epileptic hippocampus. J. Neurosci 30, 16249–16261. [PubMed: 21123571]

Jacobs J, et al., 2008 Interictal high-frequency oscillations (80–500 Hz) are an indicator of seizure onset areas independent of spikes in the human epileptic brain. Epilepsia. 49, 1893–1907. [PubMed: 18479382]

Jacobs J, et al., 2010 High-frequency electroencephalographic oscillations correlate with outcome of epilepsy surgery. Ann. Neurol 67, 209–220. [PubMed: 20225281]

Jacobs J, et al., 2012 High-frequency oscillations (HFOs) in clinical epilepsy. Prog. Neurobiol 98, 302–315. [PubMed: 22480752]

Jefferys JGR, et al., 2012 Mechanisms of physiological and epileptic HFO generation. Prog. Neurobiol 98, 250–264. [PubMed: 22420980]

Jirsch J, et al., 2005 High frequency activity (100 to 500 Hz) in areas of ictal onset and propagation in patients with focal seizures. Epilepsia. 46, 267.

Jiruska P, et al., 2010 Epileptic high-frequency network activity in a model of non-lesional temporal lobe epilepsy. Brain. 133, 1380–1390. [PubMed: 20400525]

Lévesque M, et al., 2011 High-frequency (80–500 Hz) oscillations and epileptogenesis in temporal lobe epilepsy. Neurobiol. Dis 42, 231–241. [PubMed: 21238589]

Lévesque M, et al., 2012 Two seizure-onset types reveal specific patterns of high-frequency oscillations in a model of temporal lobe epilepsy. J. Neurosci 32, 13264–13272. [PubMed: 22993442]

Li L, et al., 2018 Extrahippocampal high-frequency oscillations during epileptogenesis. Epilepsia. 59 (epi. 14041).

Matsumoto H, Ajmone Marsan C, 1964a Cortical interictal phenomena in experimental epilepsy: interictal manifestations. Exp. Neurol 9, 286–304. [PubMed: 14145629]

Matsumoto H, Ajmone Marsan CA, 1964b Cortical cellular phenomena in experimental epilepsy: ictal manifestations. Exp. Neurol 25, 305–326.

Memarian N, et al., 2015 Ictal depth EEG and MRI structural evidence for two different epileptogenic networks in mesial temporal lobe epilepsy. PLoS One 10, eOl23588.

Menendez de la Prida L, Trevelyan AJ, 2011 Cellular mechanisms of high frequency oscillations in epilepsy: on the diverse sources of pathological activities. Epilepsy Res. 97, 308–317. [PubMed: 21482073]

Merricks EM, et al., 2015 Single unit action potentials in humans and the effect of seizure activity. Brain. 138, 2891–2906. [PubMed: 26187332]

Ogren J, et al., 2009a Three-dimensional hippocampal atrophy maps distinguish two common temporal lobe seizure–onset patterns. Epilepsia. 50, 1361–1370. [PubMed: 19054395]

Ogren JA, et al., 2009b Three-dimensional surface maps link local atrophy and fast ripples in human epileptic hippocampus. Ann. Neurol 66, 783–791. [PubMed: 20035513]

Perucca P, et al., 2014 Intracranial electroencephalographic seizure-onset patterns: effect of underlying pathology. Brain. 137, 183–196. [PubMed: 24176980]

Pitkanen A, Engel J Jr., 2014 Past and present definitions of epileptogenesis and its biomarkers. Neurotherapeutics 11, 231–241. [PubMed: 24492975]

Pitkanen A, Immonen R, 2014 Epilepsy related to traumatic brain injury. Neurotherapeutics. 11, 286–296. [PubMed: 24554454]

Reid AY, et al., 2016 The progression of electrophysiologic abnormalities during epileptogenesis after experimental traumatic brain injury. Epilepsia. 57, 1558–1567. [PubMed: 27495360]

Schmitz D, et al., 2001 Axo-axonal coupling. A novel mechanism for ultrafast neuronal communication. Neuron. 31, 831–840. [PubMed: 11567620]

Scott RC, et al., 2018 WONOEP APPRAISAL: the many facets of epilepsy networks. Epilepsia. 59, 1475–1483. [PubMed: 30009398]

Sheybani L, et al., 2018 Electrophysiological evidence for the development of a self-sustained large-scale epileptic network in the kainate mouse model of temporal lobe epilepsy. J. Neurosci 38, 3776–3791. [PubMed: 29555850]

Simon A, et al., 2013 Gap junction networks can generate both ripple-like and fast ripple-like oscillations. Eur. J. Neurosci 1–15.

Staba RJ, et al., 2002 Quantitative analysis of high-frequency oscillations (80–500 Hz) recorded in human epileptic hippocampus and entorhinal cortex. J. Neurophysiol 88, 1743–1752. [PubMed: 12364503]

Staba RJ, et al., 2004 High-frequency oscillations recorded in human medial temporal lobe during sleep. Ann. Neurol 56, 108–115. [PubMed: 15236407]

Staba RJ, et al., 2007 Increased fast ripple to ripple ratios correlate with reduced hippocampal volumes and neuron loss in temporal lobe epilepsy patients. Epilepsia. 48, 2130–2138. [PubMed: 17662059]

Staba RJ, et al., 2012 Gray matter loss correlates with mesial temporal lobe neuronal hyperexcitability inside the human seizure-onset zone. Epilepsia. 53, 25–34. [PubMed: 22126325]

Truccolo W, et al., 2011 Single-neuron dynamics in human focal epilepsy. Nat. Neurosci 14, 635–641. [PubMed: 21441925]

Valero M, et al., 2017 Mechanisms for selective single-cell reactivation during offline sharp-wave ripples and their distortion by fast ripples. Neuron. 94, 1234–1247 e7. [PubMed: 28641116]

van't Klooster MA, et al., 2011 Time-frequency analysis of single pulse electrical stimulation to assist delineation of epileptogenic cortex. Brain. 134, 2855–2866. [PubMed: 21900209]

Velasco AL, et al., 2000 Functional and anatomic correlates of two frequently observed temporal lobe seizure-onset patterns. Neural Plast. 7, 49–63. [PubMed: 10709214]

Weiss SA, et al., 2016a Ictal onset patterns of local field potentials, high frequency oscillations, and unit activity in human mesial temporal lobe epilepsy. Epilepsia. 57, 111–121. [PubMed: 26611159]

Weiss SA, et al., 2016b Ripples on spikes show increased phase-amplitude coupling in mesial temporal lobe epilepsy seizure-onset zones. Epilepsia. 57,1916–1930. [PubMed: 27723936]

Wilson CL, et al., 1998 Paired pulse suppression and facilitation in human epileptogenic hippocampal formation. Epilepsy Res. 31, 211–230. [PubMed: 9722031]

Worrell GA, et al., 2004 High-frequency oscillations and seizure generation in neocortical epilepsy. Brain. 127, 1496–1506. [PubMed: 15155522]

Worrell GA, et al., 2008 High-frequency oscillations in human temporal lobe: simultaneous microwire and clinical macroelectrode recordings. Brain. 131, 928–937. [PubMed: 18263625]

Ylinen A, et al., 1995 Sharp wave-associated high-frequency oscillation (200 Hz) in the intact hippocampus: network and intracellular mechanisms. J. Neurosci 15, 30–46. [PubMed: 7823136]

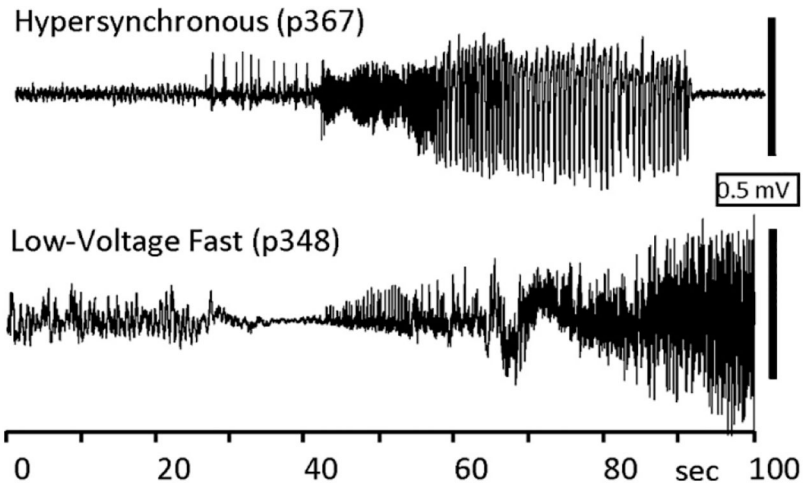

Fig. 1.

Examples of hypersynchronous (top) and low voltage fast (bottom) seizure onsets. Modified from Engel, 2013.

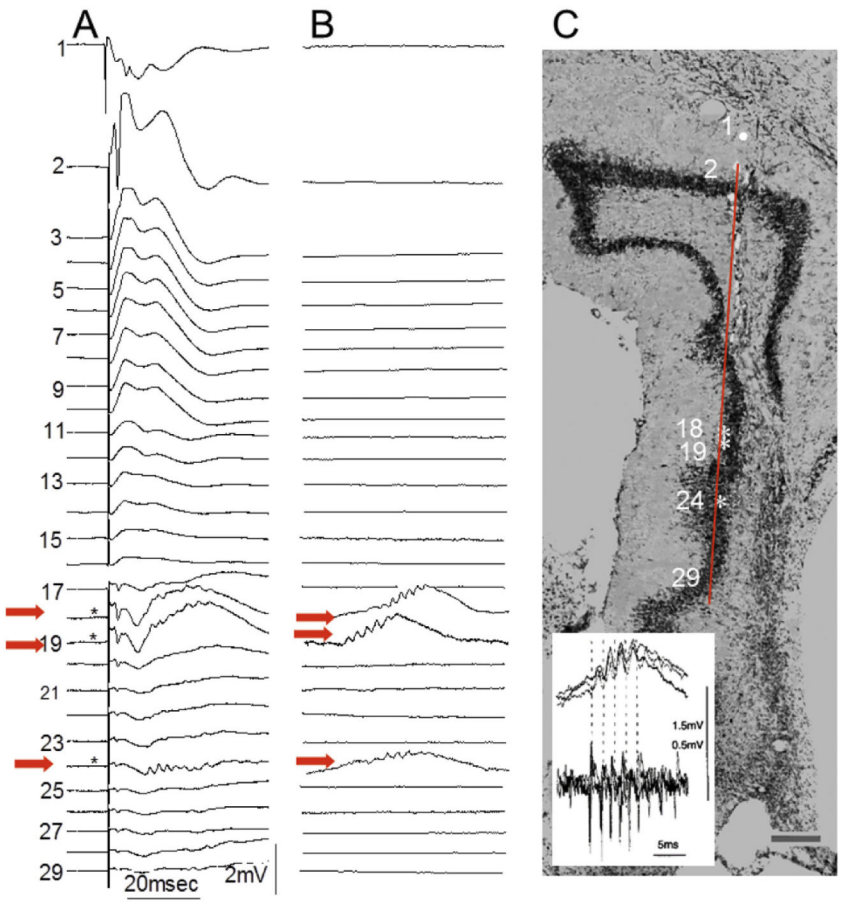

Fig. 2.

A) Voltage-depth profiles of potentials recorded at 100 μm intervals in response to perforant path stimulation. Note that FRs are evoked only at sites 18, 19, and 24. Recordings are averages of five stimulations at each side, (red arrows indicate recording sites where FR oscillations followed the initial response. B) Spontaneous FRs could be recorded only at the same sites as in A: 18, 19, and 24 (average of 5 in each trial). C) Track of the microelectrode in a Nissl-stained coronal section of the posterior curve of the hippocampus, showing the dorso-ventral extent of the dentate gyrus. Arrows indicate the beginning and the end the recording area. Stars indicate sites at which FRs were recorded. Scale bar: gray, 200 μm on the basis of histological measurement; white, 200 μm on the basis of electrophysiological measurement. Inset in part C illustrates 3 superimposed FR oscillations and discharges of neuron recorded at the same time.

Modified from Bragin et al., 2002, and Bragin et al., 1999.

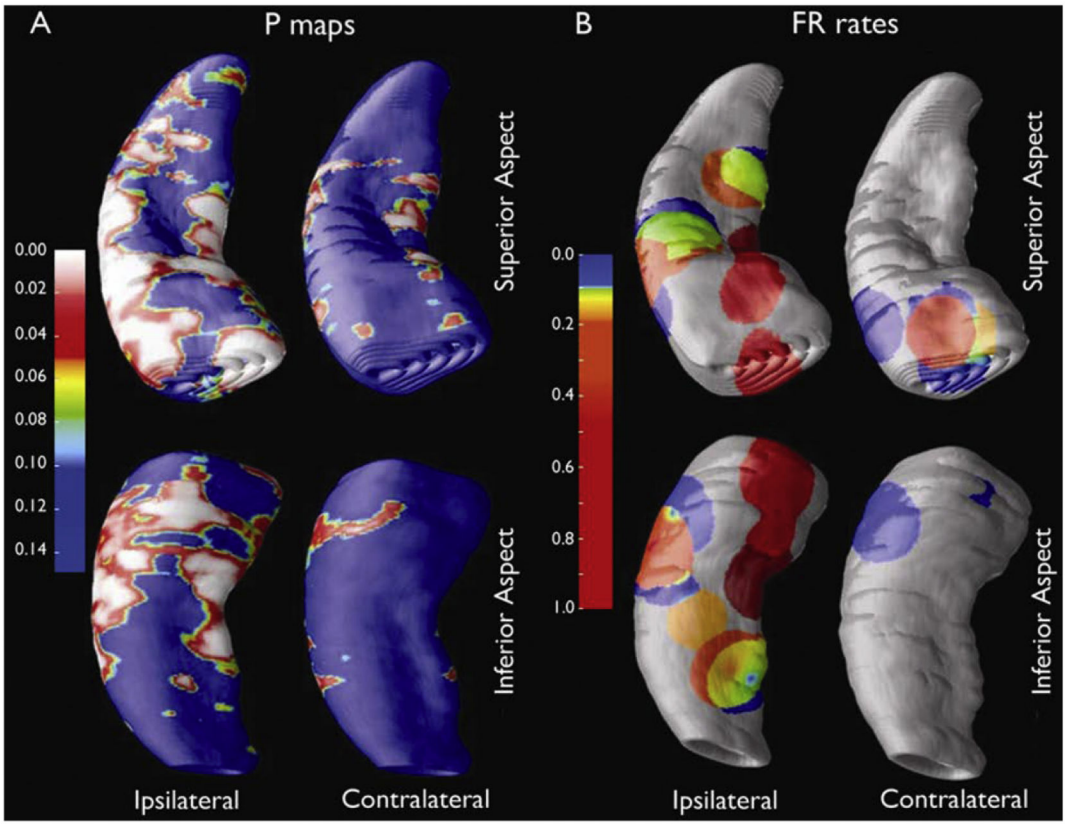

Fig. 3.

Surface contour maps of the human hippocampal formation illustrating structural and functional changes. A) Spatial pattern of hippocampal atrophy ipsilateral and contralateral to the seizure onset zone. Hotter colors white and red represents areas of significant atrophy in patients with respect to control subjects. B) Spatial distribution of the rates of fast ripple discharges recorded from microelectrodes positioned in the hippocampus. Higher rates of FR discharges correlate with local areas of hippocampal atrophy.
Modified from Ogren et al., 2009b.

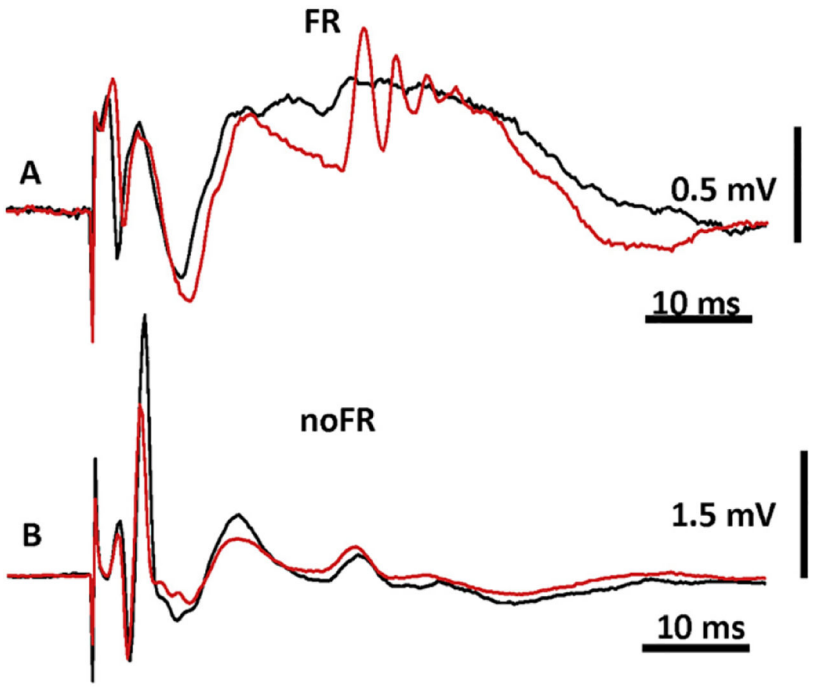

Fig. 4.

In vivo study of paired-pulse suppression of dentate gyrus population spikes in an epileptic rat in response to perforant path stimulation. A) Examples of the evoked field potentials to the conditioning (black line) and test (red line) pulses delivered with an interpulse interval of 500 msec in an area generating spontaneous FRs. B) Similar recording as in panel A, but in an area not generating spontaneous FR. Note that FR oscillations become augmented in response to the test pulse at interpulse intervals of 70–500 msec.

Modified from Bragin et al., 2002.

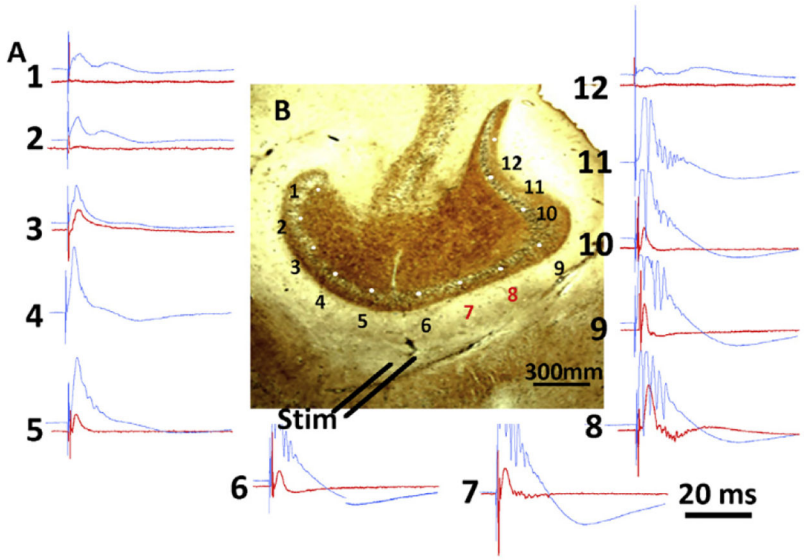

Fig. 5.

A) Areas in the in vitro dentate gyrus generating FR-like responses in normal ACSF (red lines) and after the addition of 10 M bicuculline to the perfusate (blue lines). B) Timm's-stained section demonstrating sprouting of mossy fibers in the inner molecular layer in relation to the positions of the recording sites (white dots) that were stimulated (stim) to evoke the field potentials shown in A.

Modified from Bragin et al., 2002.

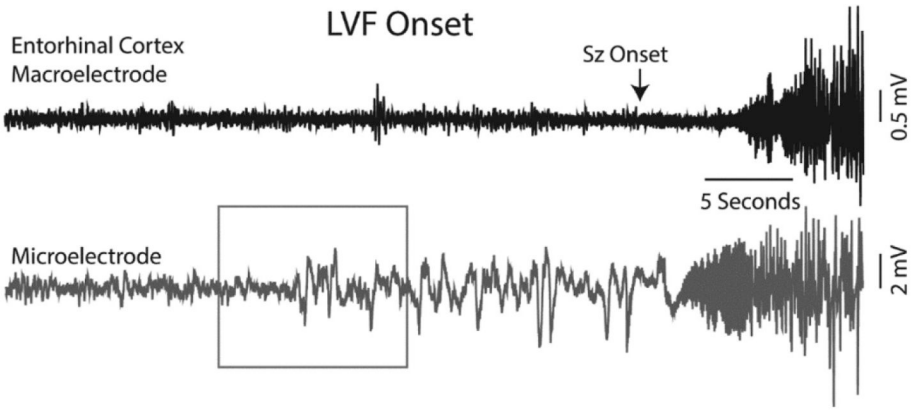

Fig. 6.

The LVF ictal onset recorded with clinical electrode in entorhinal cortex (top) is preceded by a HYP-like ictal onset recorded with microelectrodes (bottom, box). Note the microelectrode-recorded HYP onset was also associated with an increase in pHFO discharges.

Modified from Weiss et al., 2016.

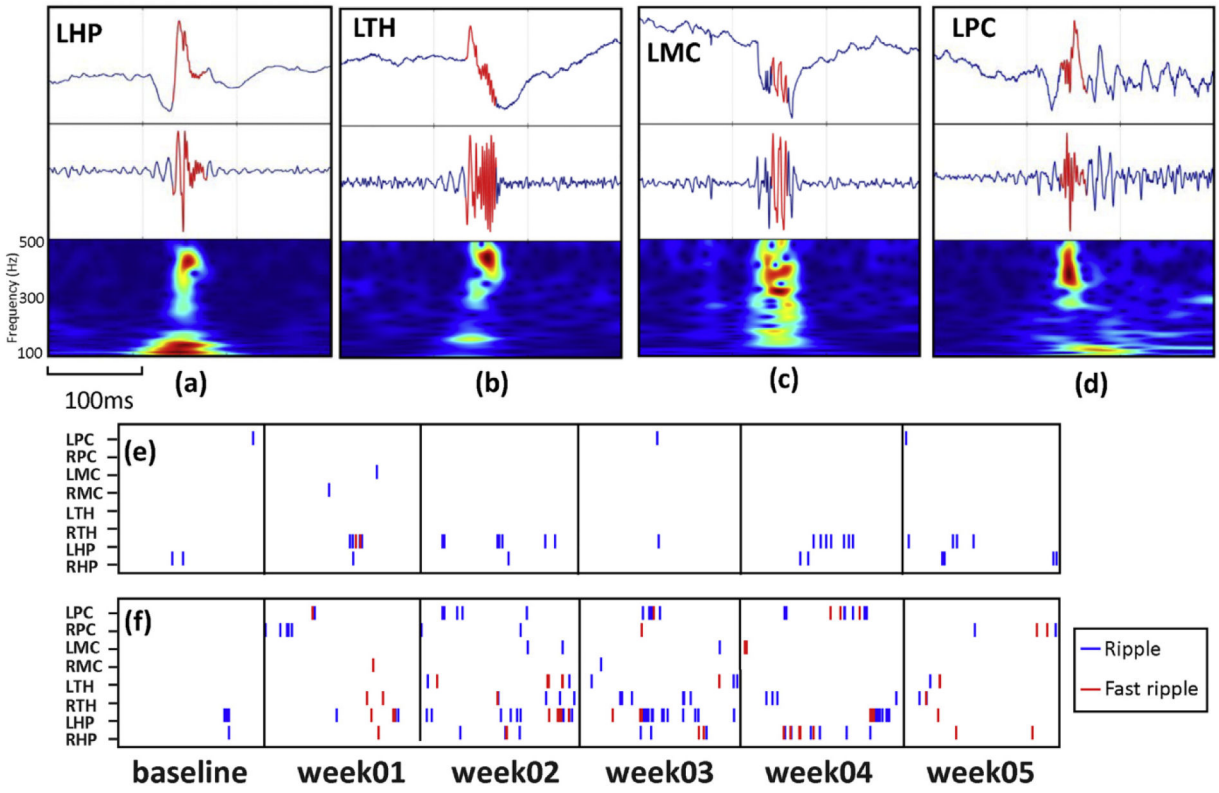

Fig. 7.

HFO events at baseline and during the 5-week latent period. A-D) Demonstration of ripples and FRs recorded by microelectrodes located in (A) left hippocampus (week 2), (B) thalamus (week 2), (C) motor cortex (week 4), and (D) prefrontal cortex (week 4) in the animals later developed epilepsy (E + group). Note that these illustrated ripples and FRs are all superimposed on large spikes (~3–10 Hz, upper plots). Data were presented as raw electroencephalographic events (300 milliseconds, upper plots), events after bandpass filter (100–500 Hz, middle plots), and their time-frequency profiles (bottom plots). A similar pattern was observed throughout the latent period in the E + group. E) & F), Demonstration of HFO events in the 8 recorded areas for the animals did not develop epilepsy (E− group) and E + group, with the illustration of ripples (blue) and FRs (red) as the bin-bars. A 10-min time frame was chosen from the combination of each animal in each group in each week. After status epilepticus, the lesion site (left hippocampus [LHP]) demonstrated continuous ripples events across all 5 weeks in both groups. Meanwhile, there was an obvious increase and spread of ripples and also FRs in the E + group in most of the remote recording sites during the entire latent period, but not in the E− group. LMC, left motor cortex; LPC, left prefrontal cortex; LTH, left thalamus; RHP, right hippocampus; RMC, right motor cortex; RPC, right prefrontal cortex; RTH, right thalamus.

Modified from Li et al., 2018.

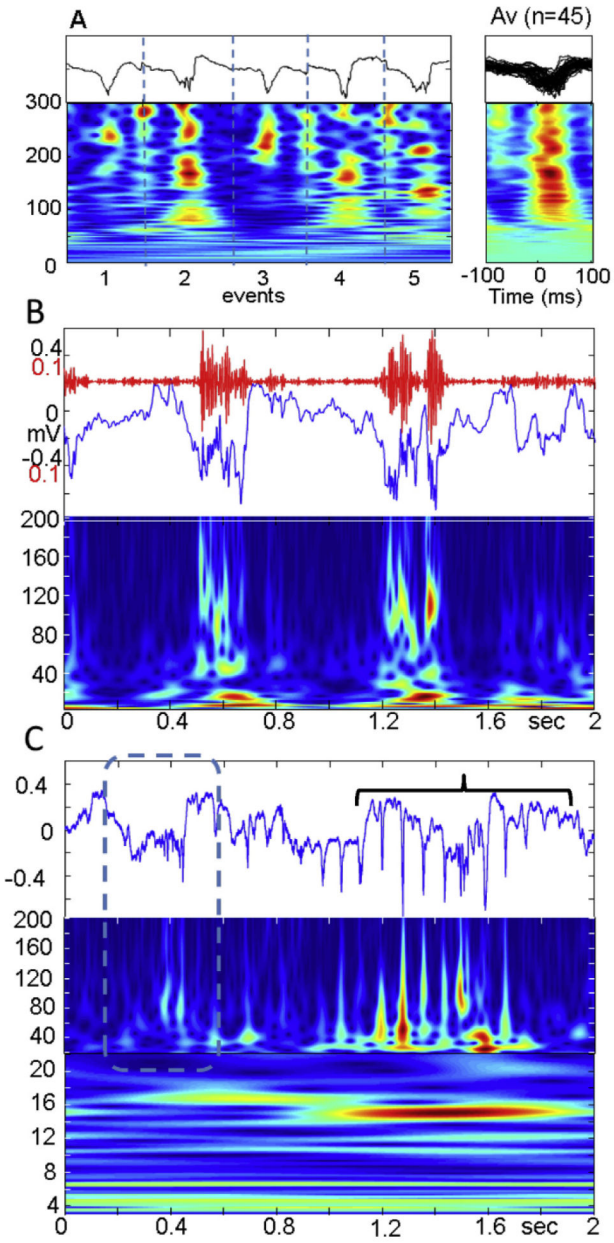

Fig. 8.

pHFOs in the neocortex 3 days after FPI. A) Five individual examples (black lines) and time frequency plots (below). (Right) time frequency plots of 45 pHFOs. B) An example of pHFOs associated with a local slow-wave. C) HFO (dashed box) followed by rHFOS (bracket) containing popSpikes.

Modified from Bragin et al., 2016.

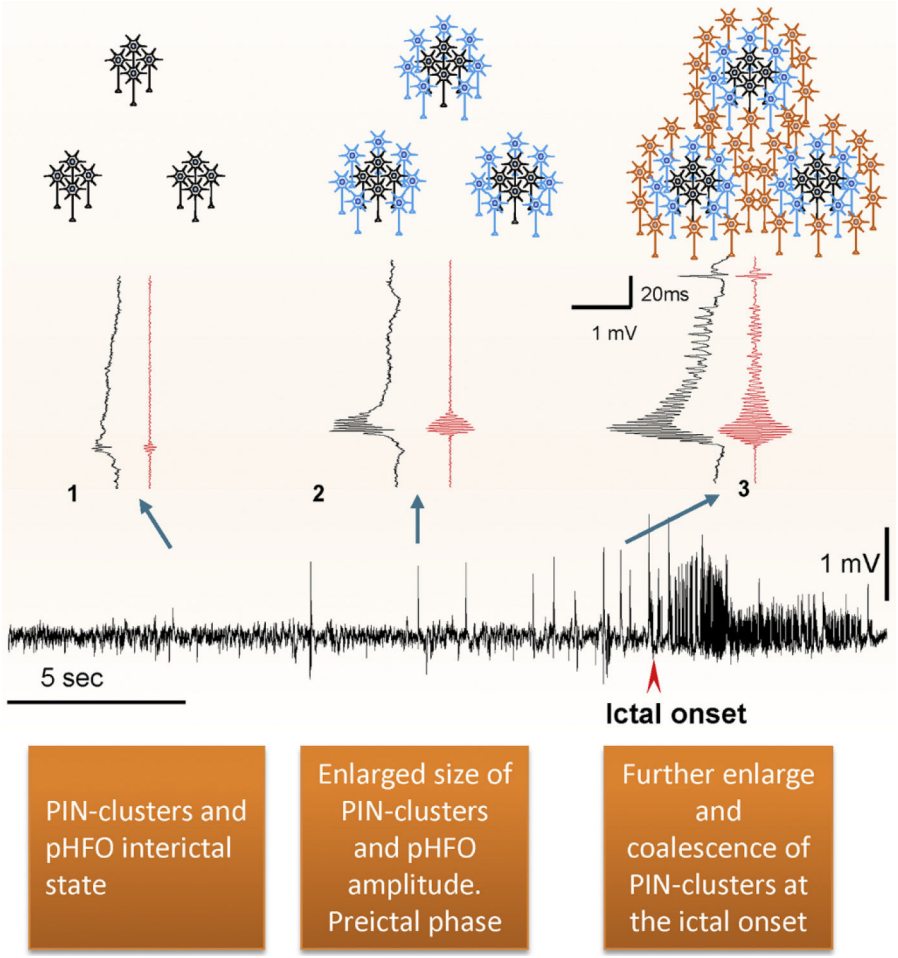

Fig. 9.

Schematic illustration of increase of PIN clusters size at the seizure onset. From the left to the right the size of PIN clusters during interictal period.

Modified from Bragin et al., 2005.